

Cohesive fracture modelling of overload effects in fatigue

V. R. Krishnan¹ and K. D. Papoulia²

¹*Theoretical & Applied Mechanics, Cornell University, Ithaca, NY, USA*

²*Civil & Environmental Engineering, University of Waterloo, Waterloo, ON, Canada*

Abstract

A cohesive fracture model is used to capture the effect of a single peak overload in a ductile 316L steel alloy under plane stress conditions, viz. crack retardation. Previously, the model was used to capture the fatigue life at different loading ratios. The model follows a bi-linear traction-displacement relationship coupled with a nonlinear damage evolution equation. The rate of damage evolution is characterized by three material parameters corresponding to damage accumulation, crack closure and stress threshold. The results indicate that a higher peak load results in higher fatigue crack retardation. The results also agree with experiments that suggest that strain hardening, not crack closure, is the leading mechanism for the overload effect.

1 Introduction

The fatigue life of a structure is influenced by mechanical, microstructural and environmental factors, all of which result in material damage, typically equated to crack length [5]. Indeed the field of fracture mechanics has had profound influence on fatigue analysis. For mechanical type loads, fatigue life of a component or structure is calculated as the number of loading cycles needed to grow a pre-existing crack to a predetermined critical dimension or to nucleate and grow a crack from a notch or other location of stress concentration.

The focus of this paper is the so-called stage-II fatigue crack growth, i.e., the stable propagation of a dominant crack. Starting with the Paris model [10, 11], fatigue life predictions have typically been based on equations relating the stage-II rate of crack growth (da/dN) to the stress intensity range (ΔK), also called the driving force, characteristic of a constant magnitude cyclic applied load and of specimen geometry. Here a is the crack length and N is the number of loading cycles. Attempts to incorporate more complex conditions affecting the crack growth rate led to models whose parameters depend on characteristics of the applied load or of the environment, as well as the redefinition of ΔK .

The Paris model and similar approaches are valid under the ideal conditions of linear elastic fracture mechanics (LEFM), small-scale yielding, constant amplitude cyclic loading and long cracks. When these conditions are not met, these approaches lose their predictive capability. In particular, the Paris model is not useful if the load is not purely cyclic or is of variable amplitude. Overload is a particular example of a varying-amplitude load. In overload, a single loading cycle has higher amplitude than all the others. It is known that the response to overload is a short-lived increase in crack speed followed by a prolonged

decrease in the speed. Our aim is to capture this behavior in our model without any additional ad hoc parameters or equations.

Cohesive zone fatigue models have most commonly been implemented as cohesive interface finite elements. De Andres *et al.* [1] proposed a bilinear traction-separation relationship, which unloads to the origin with no cyclic degradation of either the stiffness or the peak traction. Nguyen *et al.* [6] pointed out that such a model can lead to plastic shakedown that arrests crack growth after a few cycles. Hence, a distinction between loading and unloading paths is necessary, which allows for subcritical crack growth. In [6], a cohesive model with an unloading-reloading hysteresis was developed. In this work, the stiffness and the peak load degrade proportionally to the unloading stiffness as the number of cycles increases. Roe and Siegmund [12] introduced a damage variable, whose evolution resulted in the degradation of the cohesive zone traction. The cohesive relationship under monotonic loading was based on the potential proposed by Xu and Needleman [17]. Maiti and Geubelle [4] proposed a cohesive model of fatigue fracture in polymeric materials in which the cohesive stiffness evolves as a function of the rate of opening displacement and of the number of loading cycles since the onset of failure.

The proposed cohesive zone model, an earlier form of which was presented in [14], is bilinear under monotonic loading and shows a degrading peak traction and stiffness behavior under cyclic loading due to an evolving damage variable. The model is a constitutive relationship of the material, i.e., unlike the Paris and other models, its parameters do not depend on loading characteristics such as the load ratio, defined as the ratio of minimum to maximum load. Rather, it contains three physically motivated parameters, which govern crack advance, threshold, and retardation, respectively. As in [12], the model introduces a scalar (energy like) damage variable, governed by an evolution equation, which provides a phenomenological framework to account for the nonlinear processes associated with fatigue failure. Our earlier work [13] showed the ability of the model to capture crack retardation due to load ratio and healing.

2 A damage-based cohesive model allowing for crack retardation

We postulate a degrading linear traction-separation relationship of the form

$$T = F(\kappa)\delta, \tag{1}$$

where κ is a damage variable, δ is the effective opening displacement, defined in Section 3, and T is a scalar effective cohesive traction, also defined in Section 3. The dependence of

the elastic coefficient F on κ is specified by

$$F(\kappa) = \frac{\sigma_c(1 - \kappa)}{\kappa(\delta_u - \delta_c) + \delta_c}; \quad (2)$$

δ_c is the critical displacement at which the crack initiates and damage starts to accumulate, δ_u is the failure displacement, i.e., the displacement at which the traction becomes zero, and σ_c is the initial peak traction of the interface. The traction T is also required to satisfy the inequality $T \leq C(\kappa)$, where $C(\kappa)$ is specified by

$$C(\kappa) = \sigma_c(1 - \kappa). \quad (3)$$

Under cyclic loading, the model exhibits a degrading peak traction, i.e., a decreasing value of $C(\kappa)$, and a degrading stiffness, i.e., a decreasing value of $F(\kappa)$ as the value of κ increases, resulting in eventual loss of load transmission ability of the interface. The variable κ takes values between 0 and 1 corresponding to no damage and complete fracture, respectively. The expression proposed in (2) has the desirable property that the elastic coefficient $F(\kappa)$ is strictly decreasing so that the traction T decreases from σ_c (when $\kappa = 0$) to 0 (when $\kappa = 1$.) The ascending and descending linear branches of the monotonic response are not explicitly defined by the above equations but rather are a consequence of these equations. On the ascending branch, the relationship $T = F(\kappa)\delta$ holds with $\kappa = 0$ and hence $F(\kappa)$ is a fixed constant. Therefore, the relation between T and δ is linear on the ascending branch. When the opening displacement is increasing and T is at its capacity (i.e., the critical traction σ_c is attained), the inequality $T \leq C(\kappa)$ becomes binding and the equation $F(\kappa)\delta = C(\kappa)$, arrived at by substituting $T = C(\kappa)$ into (1), holds. Upon substituting (2) and (3), this yields $\delta = \kappa(\delta_u - \delta_c) + \delta_c$. Thus, the choice of (2) results in a linear relationship between κ and δ on this branch of the loading curve. Furthermore, substituting (3) shows that T , κ , and δ are all linearly related. Fig. 1 shows a schematic representation of the proposed cohesive traction-displacement relationship. In this figure, branch OB is the ascending part of the loading curve, BC is the descending part of the loading curve, and CO is the unloading curve.

The evolution of the damage variable is governed by:

$$\begin{aligned} \dot{\kappa} &= \alpha^* \kappa (T - \beta C)(\dot{\delta}) & \text{if } (T - \beta C)(\dot{\delta}) > 0, \\ \dot{\kappa} &= 0 & \text{if } (T - \beta C)(\dot{\delta}) < 0, \\ \dot{\kappa} &= \dot{\lambda} & \text{if } T = C \text{ and } \dot{\delta} > 0. \end{aligned} \quad (4)$$

where $\dot{\lambda}$ is a free variable, and α^* , β are material parameters that capture the rate of damage evolution, and the threshold for initiation of damage, respectively. The parameter α^* takes on one of two distinct values for the cases of loading and unloading, $\dot{\delta} > 0$ or

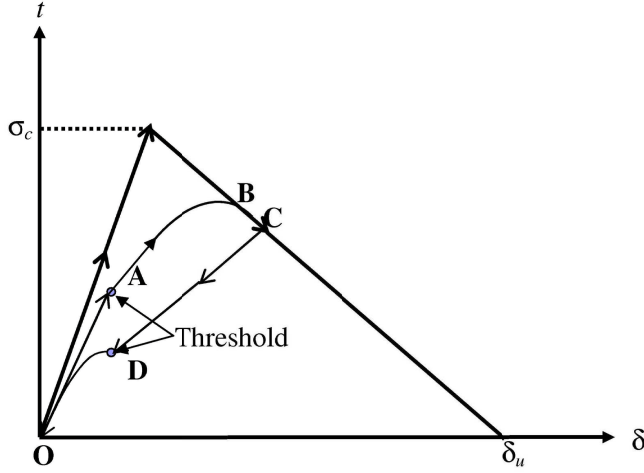


Figure 1: Schematic representation of the proposed cohesive traction-separation relationship. No change in damage occurs during OA; damage starts increasing after the threshold at A; BC shows the descending part of the loading curve; no damage change takes place during the unloading path CD; damage decreases during unloading from D to O.

$\dot{\delta} < 0$, denoted by the parameters α and $-\gamma$, respectively, which are regarded as material parameters.

Evolution equations (4) are reminiscent of damage plasticity [3]. The first and second equations allow damage accretion (when $\dot{\delta} > 0$) or healing (when $\dot{\delta} < 0$) to occur only when the traction is greater or less than the threshold limit during loading and unloading, respectively. Physically, this can be thought of as damage accretion or healing occurring only when the work done by an effective traction, i.e., the value of the traction above the threshold, on the crack surface is positive. A key property of both surface roughness and crack tip plasticity as causes of crack retardation is that they become strongly active only when the crack opening displacement returns to a small value in the trough of the cyclic loading. This explains why our evolution equation for damage decrease is inactive until the traction drops below a threshold level. During loading, if the value of the traction (T) reaches peak traction (C), it is constrained to move along the envelope $T = C(\kappa)$. This in turn forces the relationship $C(\kappa) = F(\kappa)\delta$ to hold, which defines the evolution of κ . Therefore, for this situation, the third case of (4) does not constrain $\dot{\kappa}$ at all since $\dot{\lambda}$ is free. This case is again analogous to classical plasticity theory in which a parameter $\dot{\lambda}$ is chosen in the loading case to ensure that the stress remains on the yield surface. The analogy to plasticity is not complete, however, because our model does not involve a strain or relative displacement decomposition.

3 Finite Element Implementation and Extrapolation

The cohesive model described in Section 2 is implemented as a constitutive relationship governing interface elements in a finite element mesh. These are zero thickness elements obtained by duplicating grid points along bulk element edges. Our cohesive finite element implementation, which is based in part on work by Ortiz and Pandolfi [7], depends on an effective scalar parameter

$$\delta = \sqrt{\eta^2 \boldsymbol{\delta}_s \cdot \boldsymbol{\delta}_s + \delta_n^2}, \quad (5)$$

where η is a nondimensional factor that couples the normal and shear effects, $\boldsymbol{\delta}_s$ is the shear component of the opening displacement and δ_n is the normal component. The cohesive model (1) defines a scalar traction T as a function of effective opening displacement. This scalar traction is used in turn to define the usual vector traction via the formula:

$$\mathbf{t} = \frac{T}{\delta} (\eta^2 \boldsymbol{\delta}_s + \delta_n \mathbf{n}). \quad (6)$$

Following standard procedures, e.g., [17, 7], the finite element discretization is obtained from a virtual power equation that involves power due to stresses in the bulk material and power due to interface tractions. Because of the ascending branch of the cohesive model, which makes the model active before the critical stress is reached, node duplication is necessary from the outset of the simulation. In cases where the crack path is not known in advance, cohesive interface elements must tile the domain. This results in mesh dependence associated with the ascending stiffness of the cohesive model [2]. On the other hand, implementation of cohesive interface elements that are inactive (rigid) before the critical stress is reached [7, 8], and therefore can be inserted adaptively as needed, is not easy in implicit calculations. However, all applications in this paper involve a predetermined crack path so that cohesive interface elements are inserted along that path only and the effect of the ascending stiffness is minimal. Likewise, the obvious mesh dependence of interface finite elements is avoided without need of any special meshing strategies [9].

Cycle-by-cycle simulations of high-cycle fatigue applications require excessive computational resources. For this reason, a simple but quite effective extrapolation scheme was used to predict the fatigue life of the specimens. Suppose one wishes to simulate N cycles of a material whose fatigue parameters in our model are (α, β, γ) . Suppose also that a damage-accumulation scaling function $f(k)$ exists such that one could instead compute only N/k cycles explicitly using modified parameters $(\alpha f(k), \beta, \gamma f(k))$. The function $f(k)$ is chosen so that one cycle with these modified parameters causes an equal amount of fatigue crack propagation as k cycles with the actual parameters. Note that the damage accumulation parameters α and γ are scaled but not the threshold parameter β . We carried out a variety of experiments with ranges of parameters and crack lengths and found that in all cases, linear scaling with $f(k) = k$ gave excellent results, i.e., N cycles with (α, β, γ)

gave very similar results as N/k cycles with $(\alpha k, \beta, \gamma k)$. Note that the scaling is purely an extrapolation scheme and is not a change of the model parameters.

The model was implemented in the finite element software Abaqus. All analyses were performed under the assumption of plane strain. Each explicit cycle for the $R = 0.1$ simulation had 18 time steps and the $R = 0.1$ simulation had 10 time steps per load cycle. This was chosen so that each load step is an increment or decrement of 10% of the peak load. The fatigue parameters α , β , and γ that appear in the damage evolution equation (4) were chosen so that good agreement is obtained with the experimental crack length versus load cycle curves.

4 Overload effect

Fatigue crack growth rates are well known to be decelerated by the application of overloads, which tend to cause an initial increase of the crack growth rate, followed by fast decrease before the final return to steady state crack propagation. The cause is usually attributed to plasticity induced crack closure, strain hardening, crack tip blunting, crack deflection, and/or branching depending on the toughness of the material. Wheatley *et al.* [15] performed experiments on ductile 316L steel, which indicated that overall crack retardation under plane stress conditions is related to strain hardening and residual compressive stresses in the plastic region of the overload. Plane stress simulations using the proposed model were performed on a CT specimen of width 40 mm and thickness 6 mm [16] with an initial crack 18 mm long. In the experiment, the pre-crack was initially a 12 mm blunt crack, which facilitated a 6mm crack obtained with the application of high cycle fatigue loading. The applied loading ratio was $R = 0.1$ with a minimum load of 3 kN. An elastic-plastic material model with linear kinematic hardening was used to model the bulk material with parameters $E = 1.93$ GPa, $\nu = 0.33$, $\sigma_c = 588$ MPa, and $\sigma_y = 334$ MPa, as given in the experiment.

Figure 2 shows simulation results for several single peak overloads applied early on ($N=4,000$ cycles.) Crack retardation is more pronounced when the overload is higher. The crack accelerates immediately following the overload but slows down within a few cycles and then reaches a minimum before eventually attaining the pre-load crack growth rate. The simulations closely match the experimental results. The extrapolation scheme was applied during the constant amplitude portions of the loading, i.e., away from the overload. It was observed that using the extrapolation scheme soon after the application of the overload caused the finite element program to crash due to the sudden increase in the value of the damage variable in the process zone. Hence, cycle-by-cycle calculations.

Unlike in the cyclic loading of the aluminum alloy CT specimen described in our other work [13], surface roughness and asperities do not seem to have significant effect on the

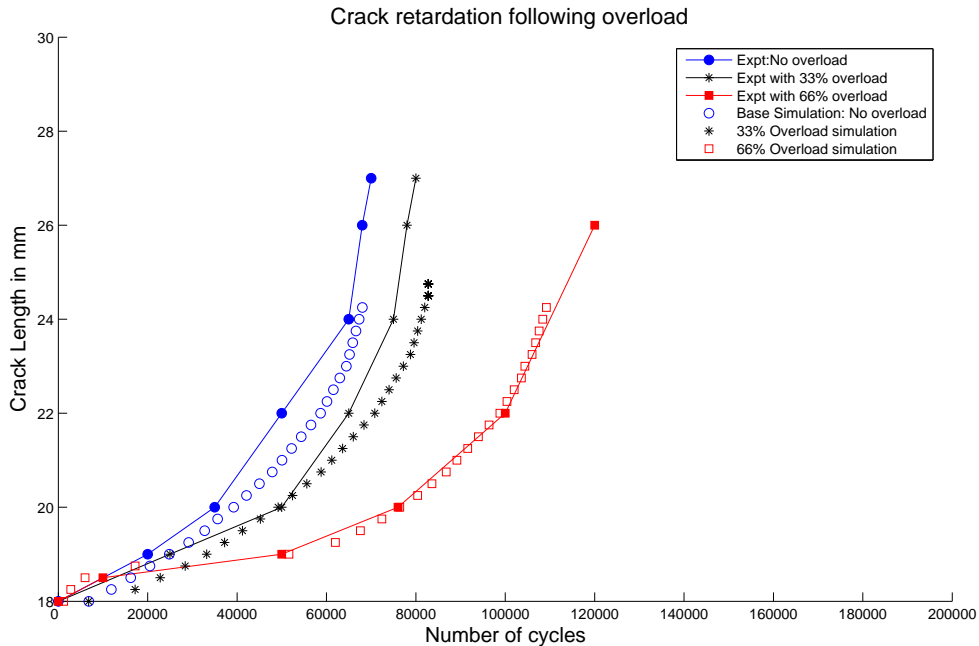


Figure 2: Illustration of overload effect : crack retardation following application of a single peak overload increases with increasing value of the peak load

crack growth rate in the present application. Based on fast scanning electron microscopy observations, Wheatley *et al.* [15, 16] suggest that strain hardening and residual stresses caused by plastic deformation due to the peak overload are responsible for crack retardation. To explain the immediate acceleration and subsequent retardation of crack growth, Wheatley *et al.* hypothesize a small fatigue damage zone ahead of the crack tip and argue that in their experiment crack closure was not a significant cause of the overload effect.

Compared to the aluminum alloy CT specimen, the plasticity zone causing crack retardation is much larger in this simulation due to the ductility of the material. Indeed, it is large enough to be represented well by plasticity of the elements in our mesh. (We confirmed the activity of the plasticity by observing a drastic change in the results when plasticity in our finite element analysis was disabled.) Thus, the cause of retardation is already captured by properties of the bulk elements, so there is no need for the γ parameter, which, as stated earlier, is intended to capture physical causes of crack retardation occurring at subgrid scales. Our FEM simulations corroborate this contention. Indeed setting γ equal to zero in the cohesive model made little difference in the crack retardation plots.

The physical interpretation is as follows: due to the sudden increase in load beyond the yield limit of the highly ductile material, strain hardening plasticity produces residual stresses in the plastic region, which envelopes the damage zone. These force the fatigue damage to be minimal and slow down the fatigue crack. Hence, even though the crack accelerates immediately following the application of the peak load due to a high value of K_{II} , the subsequent size of the damage zone ahead of the crack tip is reduced. The crack growth rate thereafter slowly increases as the size of the damage zone ahead of the crack tip increases to its pre-load value. In accordance with the theory presented in [15, 16], change in the yield stress of the material made a significant difference in the fatigue crack growth. As the ultimate stress was reduced towards a more brittle material, crack retardation was reduced to a point that it completely disappeared after the initial transient acceleration.

References

- [1] A. de Andres, J. L. Perez, and M. Ortiz. Elastoplastic finite element analysis of three-dimensional fatigue crack growth in aluminum shafts subjected to axial loading. *Int. J. Solids Structures*, 36:2231–2258, 1999.
- [2] P. Klein, J. Foulk, E. Chen, S. Wimmer, and H. Gao. Physics-based modeling of brittle fracture: cohesive formulations and the application of meshfree methods. Technical Report SAND2001-8099, Sandia National Laboratories, December 2000.
- [3] J. Lubliner, J. Oliver, S. Oller, and E. Oñate. A plastic-damage model for concrete. *Int. J. Solids Structures*, 25(3):299–326, 1989.
- [4] S. Maiti and P.H. Geubelle. A cohesive model for fatigue failure of polymers. *Engineering Fracture Mechanics*, 72(36):691–708, 2005.
- [5] K. J. Miller. Metal fatigue – past, current and future. *Proc Instn Mech Engrs*, 205:291–304, 1991.
- [6] O. Nguyen, E. A. Repetto, M. Ortiz, and R. A. Radovitzky. A cohesive model of fatigue crack growth. *International Journal of Fracture*, 110:351–369, 2001.
- [7] M. Ortiz and A. Pandolfi. Finite-deformation irreversible cohesive elements for three dimensional crack propagation analysis. *International Journal for Numerical Methods in Engineering*, 44:1267–1282, 1999.
- [8] K. D. Papoulia, C.-H. Sam, and S. A. Vavasis. Time continuity in cohesive finite element modeling. *International Journal for Numerical Methods in Engineering*, 58(5):679–701, 2003.

- [9] K. D. Papoulia, S. A. Vavasis, and P. Ganguly. Spatial convergence of crack nucleation using a cohesive finite element model on a pinwheel-based mesh. *International Journal for Numerical Methods in Engineering*, 67(1):1–16, 2006.
- [10] P. C. Paris and F. Erdogan. A critical analysis of crack propagation. *Trans. ASME. J Basic Eng.*, 85:528–534, 1963.
- [11] P. C. Paris, M. P. Gomez, and W. E. Anderson. A rational theory of fatigue. *The Trend in Eng.*, 13:9–14, 1961.
- [12] K. L. Roe and T. Siegmund. An irreversible cohesive zone model for interface fatigue crack growth simulation. *Engineering Fracture Mechanics*, 70:209–232, 2001.
- [13] A. Ural, V. R. Krishnan, and K. D. Papoulia. A cohesive zone model for fatigue crack growth allowing for crack retardation. Submitted, *Internat. J. Solids Struct.*, 2008.
- [14] A. Ural and K. D. Papoulia. Modeling of fatigue crack growth with a damage-based cohesive zone model. In P. Neittaanmäki et al., editor, *Proceedings, European Congress on Computational Methods in Applied Sciences and Engineering, ECCOMAS 2004*, Jyväskylä, Finland, July 2004.
- [15] G. Wheatley, X. Z. Hu, and Y. Estrin. Effects of a single tensile overload on fatigue crack growth in a 316L steel. *Fatigue and Fracture of Engineering Materials and Structures*, 22(12):1041–1051, 1999.
- [16] G. Wheatley, R. Niefanger, X. Z. Hu, and Y. Estrin. Fatigue crack growth in 316L stainless steel. *Key Engineering Materials*, 145-149:631–636, 1998.
- [17] X.-P. Xu and A. Needleman. Numerical simulations of fast crack growth in brittle solids. *Journal of Mechanics and Physics of Solids*, 42(9):1397–1434, 1994.